



A Journal of the Gesellschaft Deutscher Chemiker

Angewandte Chemie

GDCh

International Edition

www.angewandte.org

Accepted Article

Title: Trapping of a Highly Reactive Oxoiron(IV) Complex in the Catalytic Epoxidation of Olefins by Hydrogen Peroxide

Authors: Xenia Engelmann, Deesha D. Malik, Teresa Corona, Katrin Warm, Erik R. Farquhar, Marcel Swart, Wonwoo Nam, and Kallol Ray

This manuscript has been accepted after peer review and appears as an Accepted Article online prior to editing, proofing, and formal publication of the final Version of Record (VoR). This work is currently citable by using the Digital Object Identifier (DOI) given below. The VoR will be published online in Early View as soon as possible and may be different to this Accepted Article as a result of editing. Readers should obtain the VoR from the journal website shown below when it is published to ensure accuracy of information. The authors are responsible for the content of this Accepted Article.

To be cited as: *Angew. Chem. Int. Ed.* 10.1002/anie.201812758
Angew. Chem. 10.1002/ange.201812758

Link to VoR: <http://dx.doi.org/10.1002/anie.201812758>
<http://dx.doi.org/10.1002/ange.201812758>

COMMUNICATION

Trapping of a Highly Reactive Oxoiron(IV) Complex in the Catalytic Epoxidation of Olefins by Hydrogen Peroxide

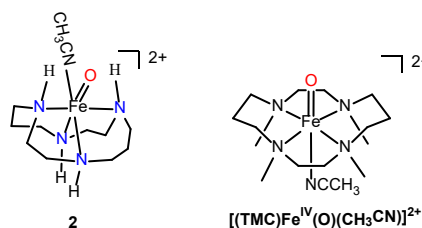
Xenia Engelmann,^[a] Deesha D. Malik,^[b] Teresa Corona,^[a] Katrin Warm,^[a] Erik R. Farquhar,^[c] Marcel Swart,^[d] Wonwoo Nam,^{*[b]} Kallol Ray^{*[a]}

Abstract: Oxoiron(IV) species are the active oxidants in catalytic oxidation reactions by nonheme iron enzymes, but have been rarely captured and/or identified as the actual oxidizing species in catalytic epoxidation or hydroxylation reactions involving synthetic nonheme iron complexes. We now report the generation of a nonheme oxoiron(IV) intermediate, $[(\text{cyclam})\text{Fe}^{\text{IV}}(\text{O})(\text{CH}_3\text{CN})]^{2+}$ (**2**; cyclam = 1,4,8,11-tetraazacyclotetradecane), in the reactions of $[(\text{cyclam})\text{Fe}^{\text{II}}]^{2+}$ with aqueous hydrogen peroxide (H_2O_2) or a soluble iodosylbenzene (sPhIO) as a rare example of an oxoiron(IV) species that shows a preference for epoxidation over allylic oxidation in the oxidation of cyclohexene. Complex **2** is kinetically and catalytically competent to perform the epoxidation of olefins with high stereo- and regioselectivity. More importantly, **2** is likely to be the reactive intermediate involved in the catalytic epoxidation of olefins by $[(\text{cyclam})\text{Fe}^{\text{II}}]^{2+}$ and H_2O_2 . In spite of the predominance of the oxoiron(IV) cores in biology, the present study represents a rare example of high-yield isolation and spectroscopic characterization of a catalytically relevant oxoiron(IV) intermediate in chemical oxidation reactions.

High-valent oxoiron species are nature's tool for catalyzing a startling array of chemical transformations, including alkane hydroxylation, olefin epoxidation, *cis*-dihydroxylation, and oxidative aromatic ring cleavage.^[1-3] Oxoiron(IV) species have been identified as the reactive intermediate responsible for various oxidation reactions in several mono- and dinuclear non-heme iron oxygenases.^[3] Parallel studies with synthetic oxoiron(IV) models of these enzymes have shown that they exhibit intriguing oxidative reactivities, which in turn have provided vital insight into the modelled enzymatic reactions.^[1] Advances in

our understanding of the mechanistic role of oxoiron(IV) intermediates in nonheme iron enzymes and synthetic accessibility of similar iron(IV) intermediates in model studies have prompted investigators to view high-valent oxoiron(IV) species as key intermediates responsible for oxygen-atom transfer to organic substrates in catalytic oxidation reactions.

However, the reactions exhibited by the model oxoiron(IV) complexes are non-catalytic, with activities falling far short of the activity of the biological catalysts.^[1,2] Furthermore, synthetic oxoiron(IV) compounds are known to prefer allylic oxidation over epoxidation of cyclohexene^[4] and are often not kinetically competent to perform the rapid oxidation observed in iron-catalyzed epoxidation and hydroxylation reactions.^[1,2] These results have previously allowed the exclusion of oxoiron(IV) species as the actual oxidizing species in chemical catalysis. In contrast, spectroscopically detected oxoiron(V) species in catalytic systems based on synthetic iron complexes bearing tetradentate N4-donor ligands with *cis*-binding sites, H_2O_2 , and carboxylic acid or water as an additive are demonstrated to be highly efficient in the selective oxidations of C-H and C=C groups of various organic substrates.^[2f,2h,2i,2j,2k,5] Thus, although the involvement of oxoiron(V) species in oxidation reactions is well-established, the intermediacy of its one-electron reduced form (i.e., oxoiron(IV) species) in catalytic oxidations by nonheme iron complexes remains elusive.



Scheme 1. Oxoiron(IV) complexes that are considered in this study

The first clean epoxidation of olefins by H_2O_2 catalyzed by a nonheme iron complex, $[(\text{cyclam})\text{Fe}^{\text{II}}]^{2+}$ (**1**; cyclam = 1,4,8,11-tetraazacyclotetradecane), was reported by Valentine and co-workers^[5a] over two decades ago. In the study, olefins were converted to the corresponding epoxides with high product yields and stereospecificity. A hydroperoxoiron(III) species was proposed as the plausible reactive intermediate without any spectroscopic evidence supporting the catalytic ability of this species for epoxidation.^[3b,5] However, no further systematic investigation on this highly intriguing catalytic olefin epoxidation system has been explored. Herein, we report the trapping and spectroscopic characterization of an oxoiron(IV) intermediate, $[(\text{cyclam})\text{Fe}^{\text{IV}}(\text{O})(\text{CH}_3\text{CN})]^{2+}$ (**2**; Scheme 1), that is kinetically and catalytically competent to perform the epoxidation of olefins at fast reaction rates and with high stereo- and regioselectivity. This

[a] Prof. Dr. K. Ray, M. Sc. X. Engelmann, Dr. T. Corona, M. Sc. K. Warm
Department of Chemistry
Humboldt-Universität zu Berlin
Brook-Taylor-Straße 2, 12489 Berlin (Germany)
E-mail: kallol.ray@chemie.hu-berlin.de

[b] Prof. Dr. W. Nam, M. Sc. D. D. Malik
Department of Chemistry and Nano Science
Ewha Womans University
Seoul 120-750, Korea
E-mail: wwnam@ewha.ac.kr

[c] Dr. E. R. Farquhar
Case Center for Synchrotron Biosciences
NSLS-II, Brookhaven National Laboratory
Upton, NY 11973, USA

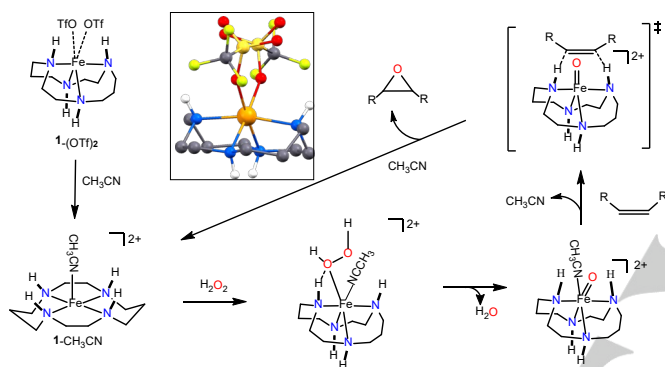
[d] Prof. M. Swart
ICREA, Pg. Lluís Companys 23, 08010 Barcelona, Spain
IQCC, Universitat de Girona, Campus Montilivi, 17003, Girona, Spain

Supporting information for this article is given via a link at the end of the document.

COMMUNICATION

is in contrast to the reactivity of the corresponding $[(\text{TMC})\text{Fe}^{\text{IV}}(\text{O})(\text{CH}_3\text{CN})]^{2+}$ (TMC = 1,4,8,11-tetraaza-1,4,8,11-tetramethylcyclotetradecane) complex (scheme 1),^[6] where all the amino functions of the cyclam ligand are methylated, which is reported to be a sluggish oxidant in oxygen-atom transfer and C-H bond oxidation reactions. In fact, **2** represents a rare example of an oxoiron(IV) species that shows a preference for epoxidation over allylic oxidation and is likely to be the reactive intermediate involved in the nonheme iron cyclam-catalyzed epoxidation of olefins by H_2O_2 .

Combination of the tetradentate cyclam ligand with $\text{Fe}(\text{OTf})_2(\text{CH}_3\text{CN})_2$ (OTf = CF_3SO_3^-) yielded the iron(II) cyclam complex, $[(\text{cyclam})\text{Fe}^{\text{II}}(\text{OTf})_2]$ (**1**- $(\text{OTf})_2$).^[5a] The X-ray structure of **1**- $(\text{OTf})_2$ displays a 6-coordinate geometry with an average Fe-N distance of 2.148(5) Å and two *cis*-positions occupied by triflate ligands (Scheme 2; Tables S1 – S2). The macrocyclic ring exhibits a *cis*-V configuration,^[7] where two out of the four -NH hydrogens are oriented *cis* to the two *cis* triflates.^[8]



Scheme 2. Role of hydrogen bonding interactions of the cyclam -NH hydrogens in the formation of **2** and its subsequent reaction with olefins. The inset shows the molecular structure of **1**- $(\text{OTf})_2$ (Fe, orange; C, grey; H, white; N, blue; O, red; S, yellow); crystal data and selected bond distances and angles are provided in Tables S1 and S2.

Table 1: Comparison of the oxidation products of cyclohexene under catalytic (0.02 mmol **1**- $(\text{OTf})_2$; 1 mmol H_2O_2 or PhIO in CH_3CN at 25 °C) and stoichiometric conditions (1 mmol **2** in CH_3CN at -20 °C).

Oxidant [ox]	Products / product yield (mmol) ¹			Yield ² [%]
	a	b	c	
Cyclohexene				
1/ H_2O_2	0.40	0.01	0.004	41
1/PhIO	0.38	-	-	38
2	0.60	0.10	0.05	75

¹The formation of diol products was not observed; ²Yield based on H_2O_2 /PhIO under catalytic conditions and based on **2** under stoichiometric conditions.

The zero-field Mössbauer spectrum (Figure S1) of **1**- $(\text{OTf})_2$ at 35 K revealed a major doublet [85%] with an isomer-shift (δ) of 0.57 mm/s and a small quadrupole splitting (ΔE_Q) of 0.41 mm/s,

demonstrating that the iron center remains in the intermediate-spin configuration ($S = 1$).^[9] The minor doublet (15%; $\delta = 0.26$ mm/s and $\Delta E_Q = 0.83$ mm/s) presumably corresponds to an iron(III) product formed in the reaction of **1**- $(\text{OTf})_2$ with traces of oxygen.

Treatment of **1**- $(\text{OTf})_2$ with a slow addition of 50 equiv H_2O_2 over a period of 1 min in the presence of excess cyclohexene in acetonitrile (CH_3CN) at 25 °C under an inert atmosphere resulted in the formation of cyclohexene oxide (40% based on H_2O_2) with a turnover number of 20 (Table 1), consistent with the previous report.^[5a] Notably, only small amounts of allylic oxidation products (2-cyclohexen-1-ol and 2-cyclohexen-1-one) were formed (Table 1), suggesting that typical radical reactions are not involved. Similarly, no dihydroxylation products were observed, which may exclude oxoiron(V) species as the actual oxidizing species in this reaction; the oxoiron(V) species have been frequently proposed as intermediates giving dihydroxylation products in the oxidation of olefins by nonheme iron catalysts and H_2O_2 .^[2f,2h,2i,2j,2k,5] When *cis*-stilbene was used as the substrate, the major product was *cis*-stilbene oxide (33% based on H_2O_2),^[5a] indicating that the epoxidation reaction is stereoselective. Replacement of H_2O_2 with iodosylbenzene (PhIO) as an oxidant also gave high yields of epoxide products (Table 1). To gain insight into the nature of the oxidant, we monitored the reaction of **1**- $(\text{OTf})_2$ with 30 equiv of H_2O_2 or a soluble iodosylbenzene derivative (2-(*tert*-butylsulfonyl)iodosylbenzene; sPhIO)^[10] and 10 equiv of cyclohexene at -40 °C in CH_3CN in a cryo-stopped-flow experiment using a diode-array UV-vis detector (Figure S2). The growth and decay of a metastable species **2** with visible absorption features at 737 nm was observed in both cases. These may point to the plausible involvement of a common reaction intermediate **2** in the **1**- $(\text{OTf})_2$ -mediated epoxidation reactions by PhIO or H_2O_2 .

Intermediate **2** could be generated in high yields in the absence of any substrates that allowed its characterization by various spectroscopic methods. First, the reaction of **1**- $(\text{OTf})_2$ with 1.5 equiv of sPhIO in anhydrous CH_3CN at -40 °C led to the immediate formation of a brownish intermediate **2** ($t_{1/2} \sim 200$ s at -20 °C) with λ_{max} (ϵ_{max}) centered at 737 nm (230 $\text{M}^{-1} \text{cm}^{-1}$) (Figure 1A). The electrospray ionization mass spectrum (ESI-MS) of **2** exhibited a signal at $m/z = 421.08$, which shifted by two-mass units when sPhI¹⁸O was used as an oxidant, possessing a mass and isotope distribution pattern consistent with a $[(\text{cyclam})\text{Fe}^{\text{IV}}(\text{O})(\text{OTf})]^{2+}$ formulation (Figure S3). However, based on NMR and X-ray absorption spectroscopy (XAS), a $[(\text{cyclam})\text{Fe}^{\text{IV}}(\text{O})(\text{CH}_3\text{CN})]^{2+}$ assignment has been concluded for **2** (Figure 1B and Figure S4C). For example, ¹⁹F NMR spectrum of $[(\text{cyclam}-d_4)\text{Fe}^{\text{IV}}(\text{O})(\text{CH}_3\text{CN})]^{2+}$ (**2**- d_4 ; cyclam- d_4 = cyclam ligand containing four -ND groups; Figure S4C) in CD_3CN shows a singlet at -78.84 ppm, which is indicative of the presence of free triflate anions.^[1k] Furthermore, ¹H-NMR spectrum of **2**- d_4 (Figure S4C) reveals 13 signals integrating to 23 protons, thereby suggesting that the *cis*-V cyclam configuration, observed in the X-ray structure of **1**- $(\text{OTf})_2$, is also present in **2** with two out of four -NH hydrogens being *cis* to the oxo ligand, which in turn is *cis* to a bound CH_3CN ligand (Scheme 1).^[8] Extended X-ray absorption fine structure (EXAFS) analysis of **2** confirmed the presence of the Fe=O unit that yields a best fit comprised of an O/N scatterer at 1.66 Å, which is assigned to an Fe=O unit, and a further shell

COMMUNICATION

of 5 O/N scatterers at 2.01 Å, which correspond to the N donors of the cyclam and CH₃CN ligands (Figure 1B; Table S3). The Fe K-edge XAS of **2** reveals a pre-edge energy of 7114.2 eV with an area of 25 units and an edge energy of 7125.0 eV, which are typical of previously reported *S* = 1 oxoiron(IV) complexes.^[1,2] Mössbauer spectrum of **2** recorded at 35 K exhibits a doublet representing approximately 85% of the total iron with δ = 0.10 mm/s and ΔE_Q = 1.09 mm/s (Figure 1D), which is close to the Mössbauer parameters of the related [(TMC)Fe^{IV}(O)(CH₃CN)]²⁺ complex (δ = 0.17 mm/s and ΔE_Q = 1.24 mm/s)^[10] and compares well to integer electronic spin systems with *S* = 1 Fe(IV) (δ range 0.01 to 0.14 mm/s).^[1,2] The remaining 15% of the signal with δ = 0.53 mm/s and ΔE_Q = 0.61 mm/s corresponds to unreacted [(cyclam)Fe^{II}(CH₃CN)₂]²⁺ complex (**1**-(CH₃CN)₂) (Table S4 and Figure S5), which exists as a minor species in a CH₃CN solution of **1**-(OTf)₂.

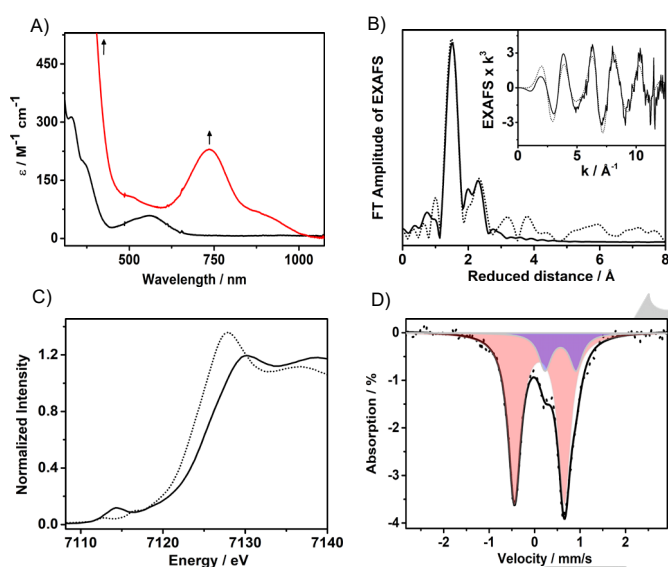


Figure 1. A): UV-vis absorption spectra of **1**-(OTf)₂ (black) and **2** (red) in CH₃CN at -40 °C. B): Fourier-transformed Fe K-edge EXAFS spectrum of **2** (experimental data, dotted line; simulation, solid line). The inset shows the corresponding EXAFS data in wave-vector scale before the Fourier transformation. C): Normalized Fe K-edge X-ray absorption spectra of **2** (black solid line) and **1**-(OTf)₂ (dashed line). D): Mössbauer spectrum of **2** recorded in CH₃CN at 35 K. The solid line is the simulation of the experimental spectrum (black dots). The major component (85%; orange shaded area; $\delta/\Delta E_Q$ = 0.10/1.09 mm/s) corresponds to **2**; the minor component (15%; purple shaded area; $\delta/\Delta E_Q$ = 0.53/0.61 mm/s) corresponds to unreacted [(cyclam)Fe^{II}(CH₃CN)₂](OTf)₂.

Replacement of sPhIO by H₂O₂ also leads to the formation of **2** (Figure S6; note that the characteristic near-IR feature in the absorption spectrum of **2** is red-shifted to 760 nm, presumably because of the binding of triflate anion in a non-coordinating solvent like acetone), albeit with a less stability and a lower yield (70%), presumably because of a subsequent reaction of nascent **2** with excess oxidant. Correspondingly, **2** could be stabilized only at -80 °C in acetone when H₂O₂ was used as an oxidant; at higher temperature, **2** decayed spontaneously to a bis(hydroxo)diiron(III) species **3** (Table S5 and Figure S7). Titration experiments confirmed a 1:1 stoichiometry between **1**-(OTf)₂ and H₂O₂ (Figure S6B). The high yield formation of **2** in the reaction of **1**-(OTf)₂ with H₂O₂ is notable in itself, since reactions of Fe(II) with H₂O₂, with

very few exceptions,^[11] afford one-electron oxidized Fe(III) products.^[2b] Energy profile for the reaction of **1**-(OTf)₂ and H₂O₂, as obtained by density functional theory (DFT) calculations (Figure S8) reveal that the transition state leading to the formation of **2** is preceded by an intermediate, where one of the cyclam-NH groups hydrogen-bonds (H-bonds) to one of the HOOH oxygens and the other HOOH oxygen is rotated away from Fe. Notably, in the absence of such H-bonding interaction, for example for the TMC ligand, where the nitrogen atoms are methylated, stoichiometric generation of the oxoiron(IV) complex using H₂O₂ as an oxidant is only possible in the presence of an externally added base.^[11c]

To understand the potential role of the oxoiron(IV) intermediate **2** in **1**-(OTf)₂-catalyzed olefin epoxidation reactions by H₂O₂ or PhIO, the reactivity of the independently generated **2** with olefins was studied experimentally (Table S6). Figure S9 shows that addition of cyclohexene to the solution of **2** in CH₃CN at -20 °C resulted in the decay of the characteristic band at 737 nm. The first-order rate constant, determined by pseudo-first-order fitting of the kinetic data for the decay of **2**, increased linearly with increasing cyclohexene concentration, thereby giving a second-order rate constant of 1.5 × 10⁻² M⁻¹ s⁻¹ at -20 °C. Product analysis of the reaction mixture revealed the formation of cyclohexene oxide (60% based on **2**) as a major product (Table 1). Some allylic oxidation products, such as 2-cyclohexen-1-ol (10%) and 2-cyclohexen-1-one (5%), were also obtained as minor products, which is in agreement with the observed preference for epoxidation over allylic oxidations under catalytic reaction conditions (vide supra).^[5a]

Reactivities of **2** with other substrates were also investigated (Table S6); a preference for epoxidation reaction was observed in each case. In particular, in the reaction with *cis*-stilbene, *cis*-stilbene oxide was the sole product, further confirming the possible involvement of **2** as a reactive intermediate in the stereoselective epoxidation reactions by H₂O₂ catalysed by **1**-(OTf)₂. In addition to epoxidation reactions, complex **2** was also capable of oxidizing a variety of substrates containing weak C-H bonds, such as xanthene, dihydroanthracene, cyclohexadiene, fluorene and indene (Figure S10). The experimentally determined second-order rate constants, *k*₂, were then adjusted for reaction stoichiometry to yield *k*₂' based on the number of equivalent target C-H bonds of substrates and correlated with the BDEs of the substrates,^[12] which gave a linear fit (Figure S10). Furthermore, a kinetic isotope effect (KIE) value of 6.7 was obtained when xanthene and xanthene-*d*₂ were used as substrates (Figure S11). These results are consistent with the rate-determining step of the reaction being C-H bond cleavage, as it is expected in hydrogen atom transfer (HAT) reactions. Product analysis of the reaction mixture for xanthene reaction revealed the formation of xanthone (64% yield) as a major product. Notably, the self-decay of **2** in the presence of excess H₂O₂ is 2 – 3 orders of magnitude faster than its reaction with substrates containing C-H or C=C bonds (Table S6; Figure S7A); correspondingly, a very slow addition of H₂O₂ is a prerequisite for achieving maximum yields of the substrate oxidation products.

Notably, the reactivity of **2** is strikingly different from that of the previously reported [(TMC)Fe^{IV}(O)(CH₃CN)]²⁺ complex,^[6] where all the amino functions of the cyclam ligand are methylated. For example, **2** performs HAT at a rate two orders of magnitude faster

COMMUNICATION

than $[(\text{TMC})\text{Fe}^{\text{IV}}(\text{O})(\text{CH}_3\text{CN})]^{2+}$ (Table S6). The greater reactivity of **2** is also reflected in the inability of $[(\text{TMC})\text{Fe}^{\text{IV}}(\text{O})(\text{CH}_3\text{CN})]^{2+}$ to perform epoxidation of olefins under catalytic reaction conditions.^[6] The higher reactivity of **2** may arise from kinetic and/or thermodynamic factors.^[13] DFT calculations (see SI for details)^[14] on the two complexes show that the Fe=O core in **2** in the experimentally determined *cis*-V configuration is sterically less hindered than in $[(\text{TMC})\text{Fe}^{\text{IV}}(\text{O})(\text{CH}_3\text{CN})]^{2+}$ (Figure S12), which would make **2** a kinetically better oxidant. Note that for both **2** and $[(\text{TMC})\text{Fe}^{\text{IV}}(\text{O})(\text{CH}_3\text{CN})]^{2+}$, a triplet $S = 1$ state has been calculated as the ground state with the excited $S = 2$ state being separated by 7.9 kcal/mol and 4.7 kcal/mol, respectively (Table S7). Thus, a two-state reactivity model^[15] cannot account for the higher reactivity of **2** as the more reactive $S = 2$ excited state is placed higher in energy in **2** than in $[(\text{TMC})\text{Fe}^{\text{IV}}(\text{O})(\text{CH}_3\text{CN})]^{2+}$. Interestingly, a KIE value of 1.4 has been determined in the epoxidation of cyclohexene, when **2-d₄** (containing four –ND groups) was employed in the reaction (Figure S13). The presence of KIE may corroborate the involvement of the cyclam–NH groups in assuring preferential epoxidation over allylic oxidation reactions in **2**. Notably, $[(\text{TMC})\text{Fe}^{\text{IV}}(\text{O})(\text{CH}_3\text{CN})]^{2+}$ and other oxoiron(IV) complexes, which lack any –NH hydrogens, undergo preferential allylic oxidation reactions.^[1,2] We presume that because of the H-bonding interaction with the cyclam –NH hydrogens, the oxidizing Fe^{IV}=O core lies in closer proximity to the C=C unit (than the –CH₂– unit) of the C=C–CH₂– substrates, thereby leading to stereo- and regioselective epoxidation reactions mediated by **2**. However, a more detailed mechanistic investigation is needed to fully understand the preference of the olefin epoxidation over the C–H bond activation in the oxidation of cyclohexene by **2**.

Catalysis systems based on iron(II) complexes of tetradentate N₄-donor ligands and H₂O₂ have attracted particular attention in the past decade due to the high efficiency and selectivity in the preparative oxidations of C=C groups of various organic molecules.^[2] High-valent oxoiron(V) species have been proposed and in few cases isolated as the reactive intermediate in these reactions.^[2f,2h,2i,2j,2k,5] In this work, we have demonstrated an oxoiron(IV) complex, **2**, as a catalytically relevant intermediate in the $[(\text{cyclam})\text{Fe}^{\text{II}}]^{2+}/\text{H}_2\text{O}_2$ catalytic system for the stereo- and regioselective epoxidation of olefins. Notably, **2** is generated as a common reactive intermediate in the reactions of $[(\text{cyclam})\text{Fe}^{\text{II}}]^{2+}$ with H₂O₂ and sPhIO, which may explain the comparable catalytic efficiency observed for both the oxidants. In spite of the predominance of the oxoiron(IV) cores in biology, the present study, to the best of our knowledge, represents a rare example where an oxoiron(IV) species has been isolated as a kinetically and catalytically competent reactive intermediate in chemical oxidation reactions. Thus, this work provides a new fundamental framework for understanding the nature of the iron-based species responsible for performing olefin epoxidation reactions in a synthetic biomimetic system that may have enzymatic relevance.

Acknowledgements

We thank the Deutsche Forschungsgemeinschaft (UniCat; EXC 314-2 and Heisenberg Professorship to KR), MINECO (CTQ2017-87392-P to MS), FEDER (UNGI10-4E-801 to MS) and

the NRF of Korea through CRI (NRF-2012R1A3A2048842 to WN) and GRL (NRF-2010-00353 to WN) for financial support. TC gratefully acknowledges the Alexander von Humboldt Foundation for a postdoctoral fellowship. XAS experiments were performed at SSRL beamline 4-1 (SLAC National Accelerator Laboratory, USA) benefited from support of the US DOE Office of Science (DE-AC02-76SF00515) and the US NIH (P30-EB-009998 and P41-GM-103393).

Keywords: Bioinorganic/Biomimetic Chemistry • Nonheme Oxoiron Intermediate • Stereoselective Epoxidation • Regioselectivity • Catalysis

- [1] a) X. Huang, J. T. Groves, *Chem. Rev.* **2018**, *118*, 2491-2553; b) R. A. Baglia, J. P. T. Zaragoza, D. P. Goldberg, *Chem. Rev.* **2017**, *117*, 13320-13352; c) X. Engelmann, I. Monte-Perez, K. Ray, *Angew. Chem. Int. Ed.* **2016**, *55*, 7632-7649; *Angew. Chem.* **2016**, *128*, 7760-7778; d) Z. Chen, G. Yin, *Chem. Soc. Rev.* **2015**, *44*, 1083-1100; e) K. Ray, F. Heims, M. Schwalbe, W. Nam, *Curr. Opin. Chem. Biol.* **2015**, *25*, 159-171; f) S. A. Cook, A. S. Borovik, *Acc. Chem. Res.* **2015**, *48*, 2407-2414; g) M. Puri, L. Que, Jr., *Acc. Chem. Res.* **2015**, *48*, 2443-2452; h) W. Nam, Y.-M. Lee, S. Fukuzumi, *Acc. Chem. Res.* **2014**, *47*, 1146-1154; i) K. Ray, F. F. Pfaff, B. Wang, W. Nam, *J. Am. Chem. Soc.* **2014**, *136*, 13942-13958; j) J. Hohenberger, K. Ray, K. Meyer, *Nat. Commun.* **2012**, *3*, 720-732; k) J.-U. Rohde, A. Stubna, E. L. Bominaar, E. Münck, W. Nam, L. Que, Jr. *Inorg. Chem.* **2006**, *45*, 6435-6445; l) M. Guo, T. Corona, K. Ray, W. Nam, *ACS Cent. Sci.* **2019**, DOI: 10.1021/acscentsci.8b00698.
- [2] a) L. Que, Jr., W. B. Tolman, *Nature* **2008**, *455*, 333-340; b) M. Milan, M. Salamone, M. Costas, M. Bietti, *Acc. Chem. Res.* **2018**, *51*, 1984-1995; c) L. Vicens, M. Costas, *Dalton Trans.* **2018**, *47*, 1755-1763; d) R. V. Ottenbacher, E. P. Talsi, K. P. Bryliakov, *Chem. Rec.* **2018**, *18*, 78-90; e) K. P. Bryliakov, *Chem. Rev.* **2017**, *117*, 11406-11459; f) R. V. Ottenbacher, E. P. Talsi, K. P. Bryliakov, *Molecules* **2016**, *21*, 1454; g) W. N. Oloo, L. Que, Jr., *Acc. Chem. Res.* **2015**, *48*, 2612-2621; h) A. Fingerhut, O. V. Serdyuk, S. B. Tsogoeva, *Green Chem.* **2015**, *17*, 2042-2058; i) O. Cusso, X. Ribas, M. Costas, *Chem. Commun.* **2015**, *51*, 14285-14298; j) A. C. Lindhorst, S. Haslinger, F. E. Kuhn, *Chem. Commun.* **2015**, *51*, 17193-17212; k) K. P. Bryliakov, E. P. Talsi, *Coord. Chem. Rev.* **2014**, *276*, 73-96; l) E. P. Talsi, K. P. Bryliakov, *Coord. Chem. Rev.* **2012**, *256*, 1418-1434; m) M. Costas, K. Chen, L. Que, Jr., *Coord. Chem. Rev.* **2000**, *200*-202, 517-544; n) S. Bang, S. Park, Y.-M. Lee, S. Hong, K.-B. Cho, W. Nam, *Angew. Chem. Int. Ed.* **2014**, *53*, 7843-7847.
- [3] a) A. J. Jasnowski, L. Que, Jr., *Chem. Rev.* **2018**, *118*, 2554-2592; b) E. I. Solomon, S. Goudarzi, K. D. Sutherlin, *Biochemistry* **2016**, *55*, 6363-6374; c) C. Krebs, D. G. Fujimori, C. T. Walsh, J. M. Bollinger, Jr., *Acc. Chem. Res.* **2007**, *40*, 484-492; d) J. C. Price, E. W. Barr, B. Tirupati, J. M. Bollinger, Jr., C. Krebs, *Biochemistry* **2003**, *42*, 7497-7508.
- [4] a) S. H. Bae, M. S. Seo, Y.-M. Lee, K.-B. Cho, W.-S. Kim, W. Nam, *Angew. Chem. Int. Ed.* **2016**, *55*, 8027-8031; b) K.-B. Cho, H. Hirao, S. Shaik, W. Nam, *Chem. Soc. Rev.* **2016**, *45*, 1197-1210; c) Y. H. Kwon, B. K. Mai, Y.-M. Lee, S. N. Dhuri, D. Mandal, K.-B. Cho, Y. Kim, S. Shaik, W. Nam, *J. Phys. Chem. Lett.* **2015**, *6*, 1472-1476; d) S. N. Dhuri, K.-B. Cho, Y.-M. Lee, S. Y. Shin, J. H. Kim, D. Mandal, S. Shaik, W. Nam, *J. Am. Chem. Soc.* **2015**, *137*, 8623-8632; e) Y. Suh, M. S. Seo, K. M. Kim, Y. S. Kim, H. G. Jang, T. Tosha, T. Kitagawa, J. Kim, W. Nam, *J. Inorg. Biochem.* **2006**, *100*, 627-633.
- [5] a) W. Nam, R. Ho, J. S. Valentine, *J. Am. Chem. Soc.* **1991**, *113*, 7052-7054; b) R. Fan, J. Serrano-Plana, W. N. Oloo, A. Draksharapu, E. Delgado-Pinar, A. Company, V. Martin-Diaconescu, M. Borrell, J. Lloret-Fillol, E. Garcia-España, Y. Guo, E. L. Bominaar, L. Que, Jr., M. Costas, E. Münck, *J. Am. Chem. Soc.* **2018**, *140*, 3916-3928; c) O. Y. Lyakin, A. M. Zima, D. G. Samsonenko, K. P. Bryliakov, E. P. Talsi, *ACS Catal.* **2015**, *5*, 2702-2707; d) J. Serrano-Plana, W. N. Oloo, L. Acosta-Rueda, K. K. Meier, B. Verdejo, E. Garcia-España, M. G. Basallote, E. Münck, L.

COMMUNICATION

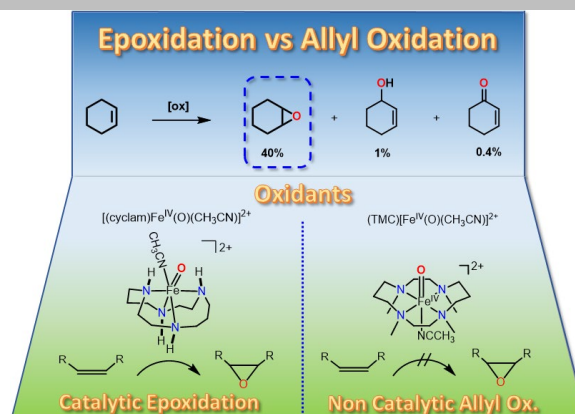
- Que, Jr., A. Company, M. Costas, *J. Am. Chem. Soc.* **2015**, *137*, 15833-15842; e) W. N. Oloo, K. K. Meier, Y. Wang, S. Shaik, E. Münck, L. Que, Jr., *Nat. Commun.* **2014**, *5*, 3046-3054; f) I. Prat, J. S. Mathieson, M. Güell, X. Ribas, J. M. Luis, L. Cronin, M. Costas, *Nat. Chem.* **2011**, *3*, 788-793; g) R. Mas-Balleste, L. Que, Jr., *J. Am. Chem. Soc.* **2007**, *129*, 15964-15972.
- [6] J.-U. Rohde, J.-H. In, M. H. Lim, W. W. Brennessel, M. R. Bukowski, A. Stubna, E. Münck, W. Nam, L. Que, Jr., *Science* **2003**, *299*, 1037-1039.
- [7] a) T. M. Hunter, I. W. McNae, X. Liang, J. Bella, S. Parsons, M. D. Walkinshaw, P. J. Sadler, *PNAS* **2005**, *102*, 2288-2292; b) B. Bosnich, C. K. Poon, M. L. Tobe, *Inorg. Chem.* **1965**, *4*, 1102-1108.
- [8] In solution, CH₃CN replaces the bound triflate ligands of 1-(OTf)₂ with a concomitant change to the *trans*-I configuration (e.g., all four -NH hydrogens *cis* to each other) to form 1-(CH₃CN), as evident from ¹H and ¹⁹F NMR spectra of 1-(OTf)₂ and [(cyclam-*d*₄)Fe^{II}(OTf)₂] (1-(OTf)₂-*d*₄) (in CD₃CN) (see Scheme 2 and Figures S4A and S4B). The *cis*-V configuration of **2** is presumably stabilized by additional H-bonding interactions of the -NH hydrogens with OTf-anion (see Table S8).
- [9] S. Yeh, K. F. Purcell, J. S. Eck, *Phys. Lett.* **1976**, *57A*, 80-82.
- [10] PhIO is insoluble in CH₃CN and hence for kinetic measurements the soluble form of iodosylbenzene (sPhIO) is used. See (D. Macikenas, E. Skrzypczak-Jankun, J. D. Protasiewicz, *J. Am. Chem. Soc.* **1999**, *121*, 7164-7165).
- [11] a) J. Bautz, M. R. Bukowski, M. Kerscher, A. Stubna, P. Comba, A. Lienke, E. Münck, L. Que, Jr., *Angew. Chem. Int. Ed.* **2006**, *45*, 5681-5684. b) C. V. Sastri, M. S. Seo, M. J. Park, K. M. Kim, W. Nam, *Chem. Commun.* **2005**, 1405-1407; c) F. Li, J. England, L. Que, Jr., *J. Am. Chem. Soc.* **2010**, *132*, 2134-2135.
- [12] Y.-R. Luo, *Comprehensive Handbook of Chemical Bond Energies*, CRC, Boca Raton, 2007.
- [13] A. Decker, J.-U. Rohde, E. J. Klinker, S. D. Wong, L. Que, Jr., E. I. Solomon, *J. Am. Chem. Soc.* **2007**, *129*, 15983-15996.
- [14] The DFT calculated Mössbauer parameters of the *cis*-V configuration of **2** ($\delta = 0.15$ mm/s and $\Delta E_0 = 0.89$ mm/s) are in excellent agreement with the experiment ($\delta = 0.10$ mm/s and $\Delta E_0 = 1.10$ mm/s). The calculated values for the corresponding *trans*-isomer are $\delta = 0.10$, and $\Delta E_0 = 1.914$ mm/s.
- [15] a) D. Usharani, D. Janardanan, C. Li, S. Shaik, *Acc. Chem. Res.* **2013**, *46*, 471-482; b) D. Schröder, S. Shaik, H. Schwarz, *Acc. Chem. Res.* **2000**, *33*, 139-145.

COMMUNICATION

Entry for the Table of Contents

COMMUNICATION

An oxoiron(IV) complex **2** is trapped and characterized as a kinetically and catalytically competent intermediate in the [(cyclam)Fe^{II}]²⁺/H₂O₂ catalytic system for the epoxidation of olefins. Complex **2** represents a rare example of an oxoiron(IV) species that shows a preference for epoxidation over allylic oxidation reactions.



Xenia Engelmann, Deesha D. Malik, Teresa Corona, Katrin Warm, Erik R. Farquhar, Marcel Swart, Wonwoo Nam,* Kallol Ray*

Page No. – Page No.

Trapping of a Highly Reactive Oxoiron(IV) Complex in the Catalytic Epoxidation of Olefins by Hydrogen Peroxide